Nationaal Lucht- en Ruimtevaartlaboratorium

National Aerospace Laboratory NLR

NLR-TP-99354

Some critical issues in developing two-phase thermal control systems for space

A.A.M. Delil

Nationaal Lucht- en Ruimtevaartlaboratorium
National Aerospace Laboratory NLR

NLR-TP-99354

Some critical issues in developing two-phase thermal control systems for space

A.A.M. Delil

Invited Keynote Lecture for the 11th International Heat Pipe Conference, Tokyo, Japan on 12-16 September 1999.

Division: Space
Issued: August 1999
Classification of title: Unclassified

Contents

1 Table
21 Figures

(23 pages in total)

This page is intentionally left blank.

Some Critical Issues in Developing Two-Phase Thermal Control Systems for Space

A.A.M. Delil
National Aerospace Laboratory NLR, Space Division
P.O. Box 153, 8300 AD Emmeloord, The Netherlands
Phone +31 527 248229; Fax +31 527 248210; E-mail adelil@nlr.nl

ABSTRACT

This invited keynote lecture discusses some critical issues concerning development of active thermal control systems for spacecraft, more precisely the development of two-phase heat transport system technology for space applications. It is shown that many investigations are being and are to be done to solve various problems. The discussions focus on the development and in-orbit technology demonstration of Capillary Pumped Loops and Loop Heat Pipes, and on thermal/gravitational scaling of two-phase heat transport systems. They include also the prediction of gravity level dependent two-phase adiabatic and condensing flow behaviour, and the creation of two-phase flow regime (pattern) maps for different gravity environments (Earth, Moon, Mars, Microgravity). Electrochemical corrosion (pitting) problems are briefly discussed also.

Key Words: Aerospace, Thermal Control, Two-Phase Flow & Heat Transfer, Evaporation, Boiling, Condensation, Microgravity, Thermal Modelling, Similitude, Dimension Analysis, Thermal-Gravitational Scaling, Loop Heat Pipe, Capillary Pumped Loop, Ammonia, Pitting Corrosion.

1. INTRODUCTION

Most space-related heat and mass transfer problems originate from:
- Absence of gravity induced behaviour differing from the normal behaviour on earth: two-phase flow and heat transport, boiling, condensation, flow pattern maps, melting, solidification, capillary electrophoresis, crystal growth, and critical point phenomena.
- Passive or active thermal control of a variety of spacecraft: earth orbiting satellites, solar and deep space probes, satellites to and possibly landing on the moon, planets or comets.
- Hostile environments, being vibrations during the launch, aerodynamic heating in ascent and descent, meteoroids impingement, vacuum, atomic oxygen, and incident radiation (UV, X-ray, particles).

To solve these problems research has been, is and will be carried out concerning:
- Passive thermal control, including the thermophysical properties of new thermal or structural materials or components: anisotropic (sheet) materials, metal and carbon fibre honeycomb sandwich panels, multilayer insulation blankets, thermal joints and interface fillers, phase change materials for thermal storage systems, heat pipes and thermo-optical coatings for radiators.
- Active thermal control, using Variable Conductance Heat Pipes (VCHP), novel heat pipes (e.g. the Electro Hydro Heat Dynamic Pipe, EHDHP), Loop Heat Pipes (LHP), Mechanically Pumped and Capillary Pumped two-phase Loops (MPL & CPL) and their components (Vapour Quality Sensors, evaporators, condensers, valves, control reservoirs, control algorithms), electrochromic radiator coatings, louvres, flexible thermal links and rotatable thermal joints for deployable and steerable radiators.
- Thermal/gravitational modelling & scaling of two-phase heat transport systems to be used to design spacecraft systems, using terrestrial test data.
- Experiments in low-gravity environments (in drop towers, during low-g aircraft flights, in sounding rockets, or in orbit). Experiments, on pool boiling and Marangoni convection, were executed during International Micro-gravity Laboratory, US Micro-gravity Payload and EUropean REtrievable CArrier flights.
- Experiments for the demonstration of two-phase technology in orbit: ESA's two-phase experiments TPX I & II, NASA's capillary pumped loop experiments CAPL 1 & 2 & 3 and the Two-Phase Flow Thermal Control Experiment TPF, the all-American loop heat pipe experiment ALPHA, the Loop Heat Pipe Flight eXperiment LHPFX, the Cryogenic Capillary Pumped Loop Flight Experiment CCPL and the Russian experiments Mars 94 & 96, Valentina and Tatyana.

This lecture will focus on two-phase heat transport system development and design supporting activities, like thermal gravitational modelling and scaling of such systems and the assessment of gravity level dependent two-phase adiabatic flow, condensation behaviour, and flow pattern mapping.

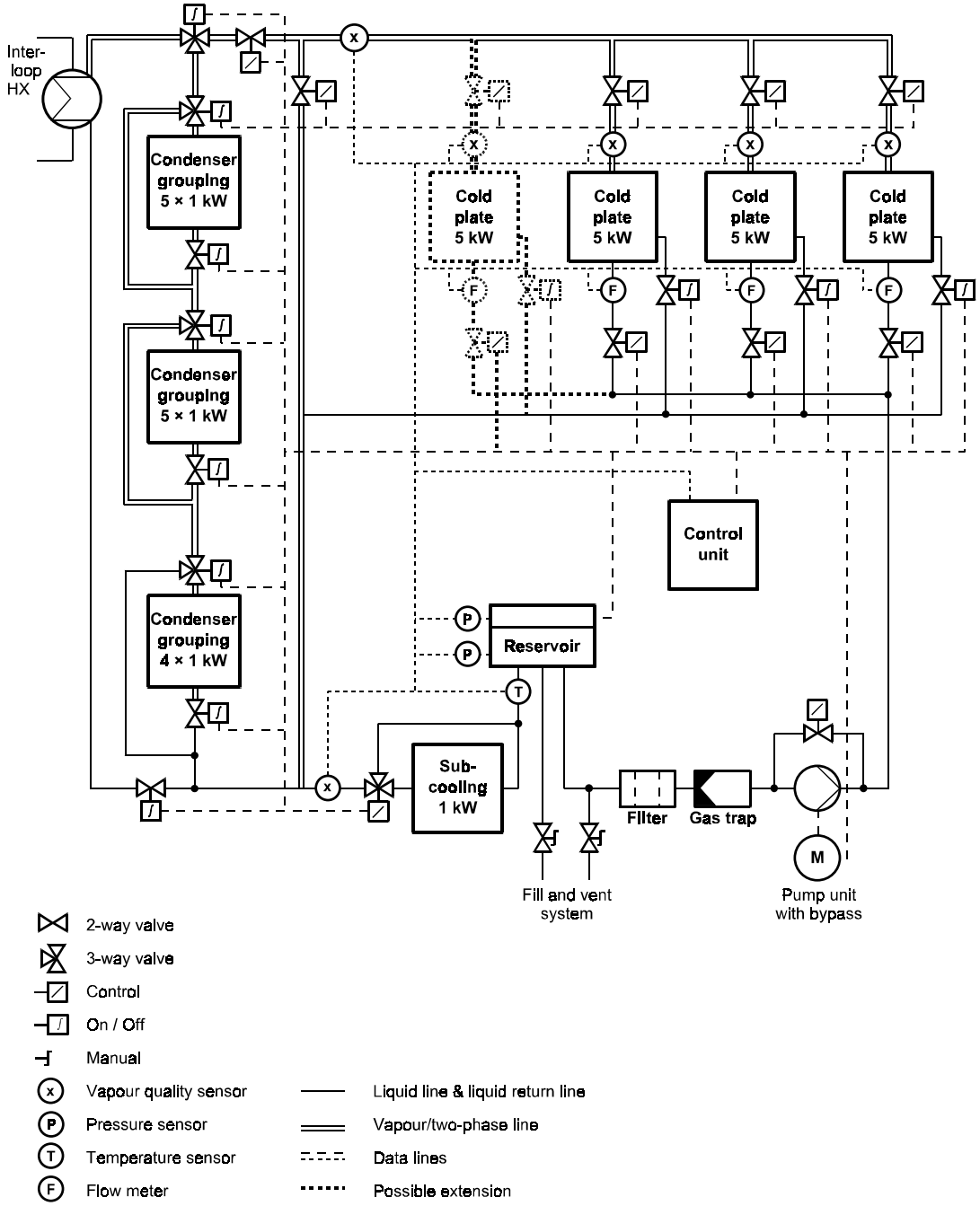

Fig.1. Schematic of ESA R114 Two-Phase Heat Transport System

2. TWO-PHASE HEAT TRANSPORT SYSTEMS

Thermal control systems for future large spacecraft must be able to transport large amounts of dissipated power (say 200 kW), over large distances (say 100 metres). Conventional single-phase systems (based on the working fluid caloric heat) are simple, well understood, easy to test, relatively inexpensive and low risk. But to realise proper thermal control with small temperature drops from equipment to radiator (to limit radiator size and mass), they require noisy, heavy, high power pumps, and consequently large solar arrays.
As an alternative for these single-phase systems one currently considers mechanically pumped two-phase systems, accepting heat by evaporation of the working fluid at heat dissipating stations (cold plates, heat exchangers), releasing heat by condensation at the heat demanding stations (hot plates, heat exchangers) and at radiators, for rejection into space. Such systems rely on the latent heat of vaporisation. They operate nearly

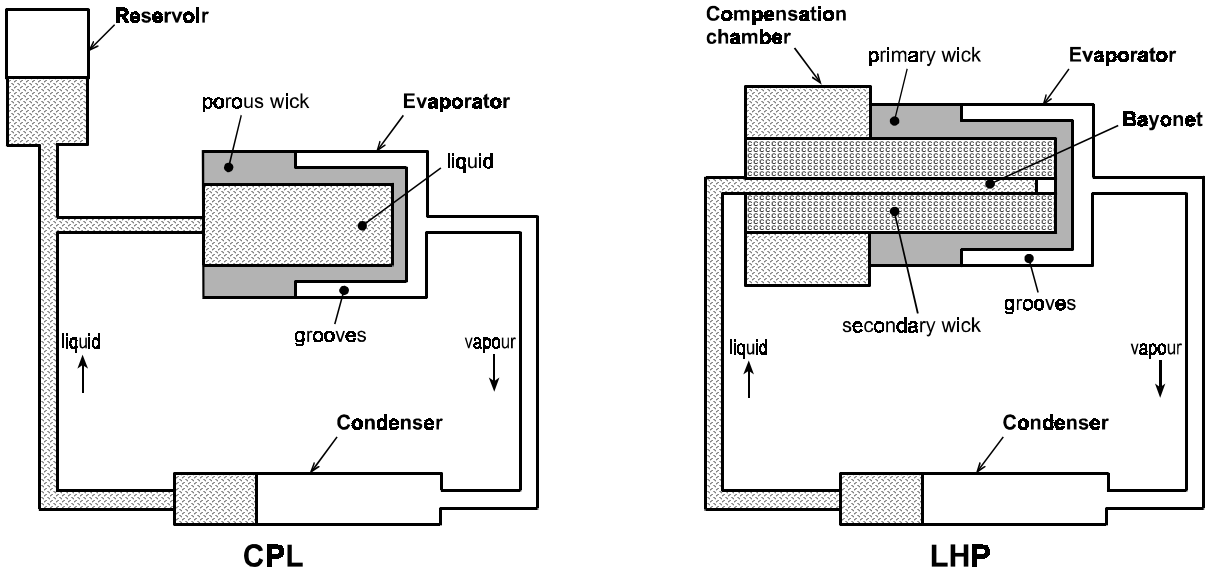

Fig.2. Schematics of Capillary Pumped Loop and Loop Heat Pipe

isothermally. Pumping power is reduced by orders of magnitude, thus minimising radiator and solar array sizes. Ammonia is the most promising candidate working fluid. The stations can be arranged in a pure series, pure parallel or hybrid configuration. The stations can be arranged in a pure series, pure parallel, or in a hybrid configuration. ESA's Two-Phase Heat Transport System TPHTS (Fig. 1) is an example of a parallel configuration. The figure shows the advantage of the concept: a modular approach, in which branches with dissipating stations (evaporators/cold plates) or heat demanding stations (condensers/radiators) simply can be added or deleted. An important future two-phase heat transport system application is the thermal control system of the Russian International Space Station segment (Cykhotsky, 1998; Ungar, 1996; Grigoriev, 1999, 1996).

Alternatives for mechanically pumped systems are capillary pumped systems, using surface tension driven pumping of capillary evaporators to transport (like in a heat pipe) the condensate back from condenser to evaporator. Such capillary two-phase systems can be used in spacecraft not allowing vibrations (induced by mechanical pumping). Ammonia is the best candidate working fluid for capillary two-phase thermal control loops also. Two different systems (Fig. 2) exist (Cullimore, Nikitkin, 1998): the western-heritage Capillary Pumped Loop, CPL (Stenger, 1966; Cullimore, 1993), and the Russian-heritage Loop Heat Pipe, LHP (Bienert, Wolf, 1995; Maidanik et al., 1991, 1995; Kaya, Ku, 1999; Ku, 1999). Active control of loop set-point temperature can be realised by control of the temperature of the reservoir or the compensation chamber, thus influencing their liquid contents, hence the amount of liquid in the rest of the loop and consequently the condenser flooding, hence the condenser area available for condensation. In this way the loop set point can be maintained independent of variations in heat load (power to be transported) or in heat sink (radiator temperature). Although initially perceived by many as alternatives to heat pipes at high transport powers (>500W, up to 24kW), in recent years the intrinsic advantages of a small-diameter piping system without distributed wick structures have been exploited at low powers (20 to 100W). Many CPL and LHP advantages are only truly exploited when these devices are considered early in the design, rather than treated as replacement for existing heat pipe based design. The advantages are:

- The tolerance of large adverse tilts (a heat source up to 4 m above a heat sink, facilitating ground testing and enabling many terrestrial applications).
- The tolerance of complicated layouts and tortuous transport paths and easy accommodation of flexible parts, make/break joints, and vibration isolation.
- Easy application in fixed conductance or variable conductance mode, fast and strong diode action.
- The separation of the heat acquisition and rejection components for independent optimisation of heat transfer footprints and even integral independent bonding of such components in larger structures.
- The accommodation of mechanical pumps.

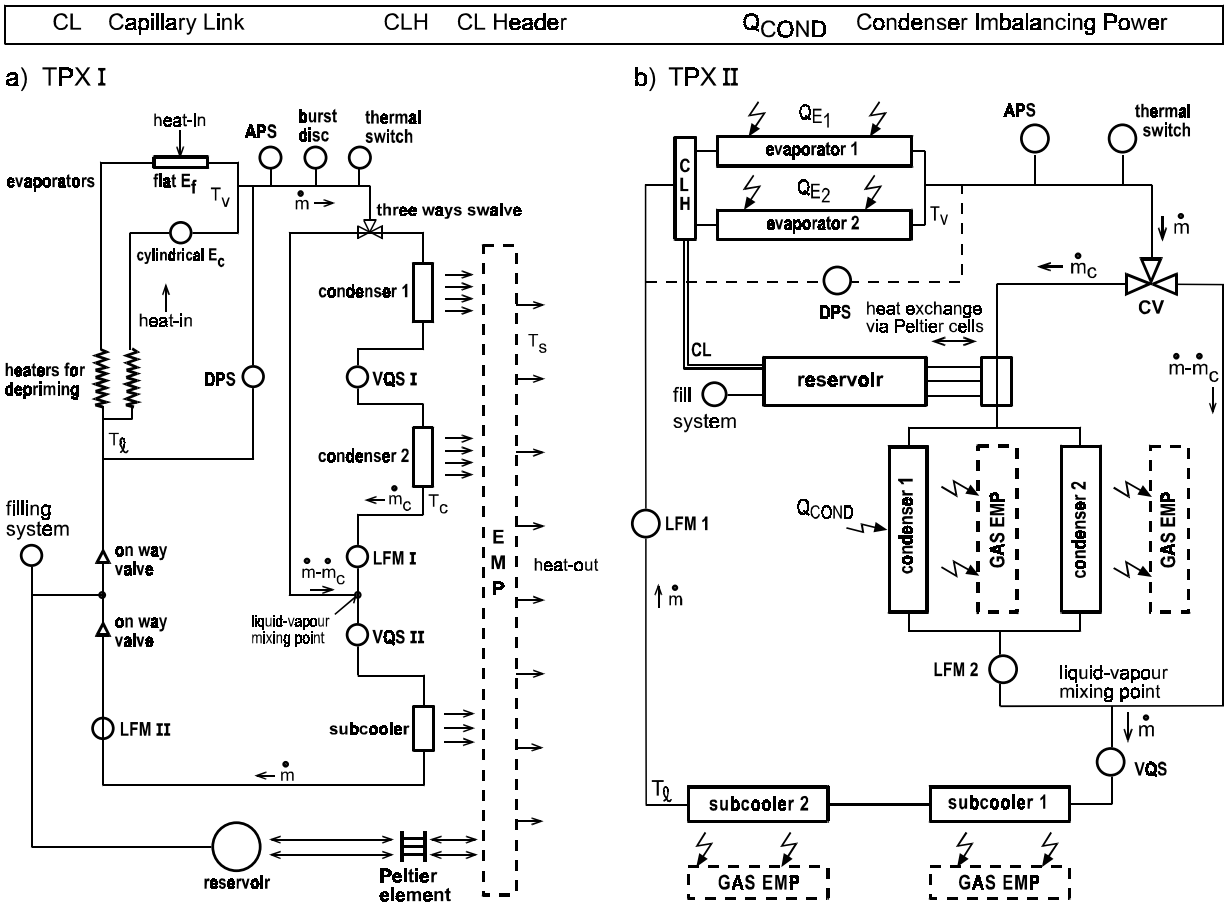

Fig. 3. TPX I & II Schematics

- An apparent tolerance of large amounts of non-condensible gases, which means extended lifetime.

Because of these performance advantages, unique operational characteristics, and recent successful flight experiments, CPLs and LHPs are currently baselined for missions in low or geo-synchronous orbits, and missions to planets (Butler, 1999). Examples are NASA's Earth Observation Satellite EOS-AM, JPL's MSP (Mars '98), ESA's ATLID, CNES's STENTOR, the Russian OBZOR and MARS 96 missions, a retrofit mission for the Hubble space telescope retrofit mission, COMET, the Hughes 702 satellites, and various other commercial communication satellites.

Since two-phase flow and heat transfer differs when subjected to earth gravity, to planetary gravity, or to microgravity environment, two-phase heat transport system technology was to be demonstrated in orbit. Therefore several in-orbit experiments were carried out. Examples are: ESA's Two-Phase eXperiment TPX I (Fig.3, Delil et al., 1995, 1997), NASA's CApillary Pumped Loop experiments CAPL 1&2 (Butler et al., 1995; Ku et al., 1996; Butler, 1999), the Loop Heat Pipe Flight eXperiment LHPFX (Bienert et al., 1998), the All US Loop Heat Pipe with Ammonia experiment ALPHA, LHP on Granat (Orlov et al., 1997) the Two-Phase Flow experiment TPF (Ottenstein, Nienberg, 1998; Antoniuk, Nienberg, 1998), and the Cryogenic CCPL (Hagood, 1998). Other in-orbit technology demonstration experiments are planned for near-term space flights.

Development supporting scientific experiments were also carried out in the last decade, within research programmes that concentrate on the physics of two-phase flow and heat transfer in microgravity (e.g. Leontiev et al., 1997). Several experiments were done in drop towers (e.g. Wőlk et al., 1999), others during Microgravity Science Laboratory missions on the Space Shuttle (e.g. Allen et al., 1999, 1998). Other investigations were executed during low-gravity aircraft flight trajectories (e.g. Lebaigue et al., 1998; Hamme, Best, 1997; Antar, Collins, 1996; Fore et al., 1996; Jayawardena, 1996; Reinarts et al., 1996, 1995, 1993; McQuilen, Neuman, 1996; Bousman, Dukler, 1994, 1993; Rite, Rezkallah, 1994; Miller et al., 1993; 1997, Zhao, Rezkallah, 1993; Huckerby, Rezkallah, 1992; Crowley, Sam, 1991; Colin et al., 1991; Kawaji et al., 1991).

3. SUPPORTING THEORETICAL WORK

3-1. Two-Phase Flow and Heat Transfer Issues

Two-phase flow is the simplest case of multiphase flow, the latter being the simultaneous flow of different phases (states of matter): gas, liquid and solid. The nature of two-phase flow in spacecraft thermal control systems is single-component, meaning that the vapour and the liquid phase are of the same chemical substance. If the two phases consist of different chemical substances, e.g. in air-water flow, the flow is called two-phase two-component flow. Flow-related (hydraulic) two-phase, single-component and two-component flows are described by the same mathematical model equations. Therefore results of calculations and experiments in one system can be used in the other, as long as they pertain to flow phenomena only, meaning that there is no heat transfer.

Heat transfer in a two-phase two-component system has a relatively simple impact on the system behaviour: only the physical (material) properties of the two phases are temperature dependent. Two-phase single-component systems are far more complicated, because the heat transfer and the temperature cause (in addition to changes of the physical properties of the phases) mass exchanges between the phases, by evaporation, by flashing and by condensation. Consequently, complicated two-phase single-component systems can not be properly understood by using modelling and experimental results of simpler two-phase two-component systems. Two-phase single-component systems, like the liquid-vapour systems in spacecraft thermal control loops, require their own, very complicated mathematical modelling and two-phase single-component experiments.

Though liquid-vapour flows obey all basic fluid mechanics laws, their constitutive equations are more numerous and more complicated than the equations for single-phase flows. These complications are due to the fact that inertia, viscosity and buoyancy effects can be attributed both to the liquid phase and to the vapour phase, and also due to the impact of surface tension effects.

An extra, and major, complication is caused by the spatial distribution of liquid and vapour, the so-called flow pattern. Figure 4 schematically shows the various flow patterns occurring in a vertical tube evaporator: the entering pure liquid gradually changes to the exiting pure vapour flow, via the main (morphological) patterns for bubbly, slug, annular and mist (or drop) flow. The hybrid flow patterns, bubbly-slug, slug-annular (churn), and annular-wavy-mist, can be considered as transitions between main patterns. It is obvious that each flow pattern (regime) requires its own mathematical modelling. In addition, transitions from one pattern to another are to be modelled also. Within a regime, further refinement of the modelling can be based on additional criteria: the relative magnitudes of the various forces or the difference between laminar and turbulent flow.

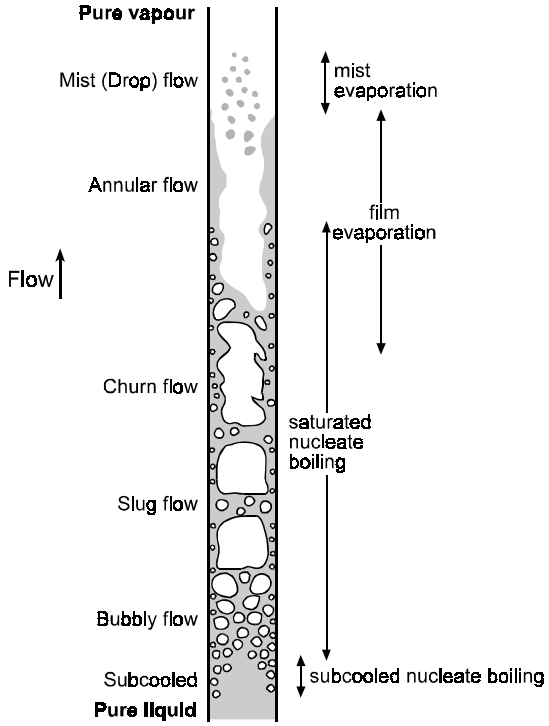

Fig. 4 Flow Patterns and Boiling Mechanisms for Up-flow in a Vertical Line

Various text books on two-phase flow and heat transfer (Wallis, 1969; Collier, 1980; Mayinger, 1982; Van Carey, 1992), derive and discuss in detail the constitutive (conservation) equations for the various (main) flow patterns, focusing on one-dimensional liquid-vapour (or gas) flow. Such one-dimensional models, especially those for homogeneous (bubbly and mist) flow, slug and annular vertical downward flow in lines of circular cross section, are relevant for the various aerospace-related two-phase issues (discussed here), as the issues for non-terrestrial gravity levels in various space environments are circular symmetric also.
By writing these equations in dimensionless form, one can identify dimensionless numbers (groups of fluid properties and dimensions) that determine two-phase flow and heat transfer. Such numbers

are very useful for similarity considerations in thermal-gravitational scaling exercises and for the creation of flow pattern maps, like the maps in the figures 5 to 7. An alternative way to derive these dimensionless numbers is by dimension analysis, constituting a useful baseline for similitude in engineering approaches, discussed in specialised text books (e.g. Murphy, 1950).

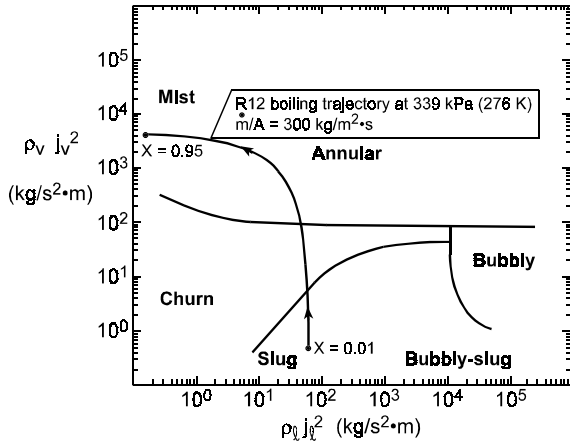

Fig. 5. Flow pattern Map for Vertical Flow

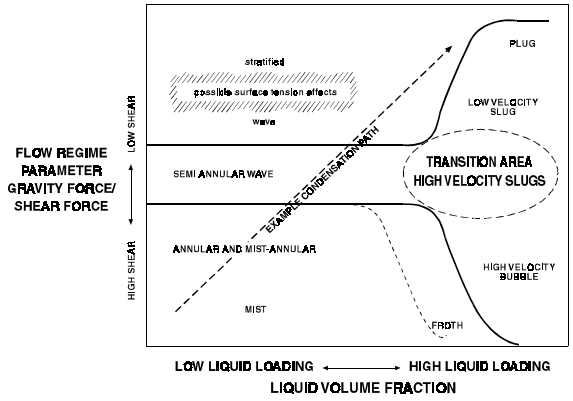

Fig. 6. Generalised Two-Parameter Flow Regime Map for Horizontal Tube Condensation

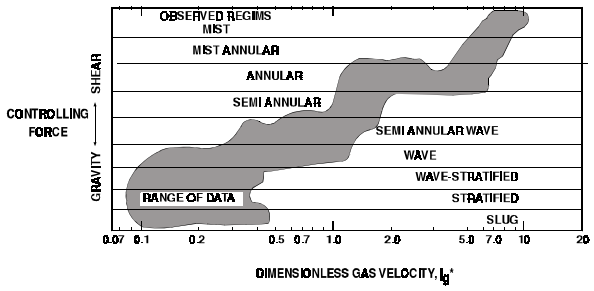

Fig. 7. Condensation Flow Regimes as Function of the Wallis, Dimensionless Gas Velocity

Anticipating the following, it can be said that the discussions here will be based on dimension-analytical considerations, assuming that:
- The homogeneous flow model is based on homogeneous mixture properties and on zero slip (equal velocities of both phases).
- The annular flow model, considering the two phases to move separately with different velocities, is valid in the adiabatic two-phase thermal control system lines, in almost the full condenser length, and also - in case of (swirl) tube evaporators - in evaporator lines.

3-2. Scaling Two-phase Flow and Heat Transfer

The modelling and scaling of two-phase heat transport systems (Delil, 1991, 1998), is done:
- For a better understanding of two-phase flow and heat transfer phenomena.
- To provide means to compare and generalise data.
- To develop a useful tool to design two-phase systems and components, to reduce costs.

Examples of the scaling of two-phase flow and heat transfer can be found in the power and in the process industry. The scaling of physical dimensions is of major interest in the process industry: large-scale industrial systems are studied by reduced scale laboratory systems. The scaling of the working fluid is of principal interest in the power industry, where large industrial systems characterised by high heat fluxes, temperatures, and pressures, are translated in full size systems, operating at lower temperature, heat flux and pressure levels (e.g. scaling a high pressure water-steam system by a low pressure refrigerant system of the same geometry).
Main goal of scaling space-related two-phase heat transport systems is the development of reliable spacecraft systems of which the proper low-gravity performance can be predicted using experimental data of scale models on earth. Scaling of spacecraft systems can be useful also:
- For in-orbit technology demonstration: the performance of spacecraft heat transport systems can be predicted using outcomes of in-orbit experiments on models with reduced geometry or different working fluid.
- To define in-orbit experiments for isolating typical phenomena to be investigated, e.g. excluding of gravity-induced disturbing buoyancy effects on alloy melting, diffusion and crystal growth, for a better understanding of the physical phenomena. The magnitude of the gravitational scaling varies with the objectives, from:
- 1 to 10^{-6} g (random direction) for the terrestrial scaling of orbiting spacecraft.
- 1 to 0.16 g for Moon, to 0.4 g for Mars systems.
- 10^{-2} or 10^{-6} g to 1 g for isolating gravity-induced disturbances on physical phenomena investigated.
- Low-g to another or the same low-g level in low-g aircraft or sounding rockets.

Table 1 Relevance of π-numbers for thermal Gravitational scaling of two-phase loops	Liquid Parts		Evaporators Swirl & Capillary	Non-liquid Lines Vapour/2-Phase	Condensers
	Adiabatic	Heating/Cooling			
π_1 = D/L = geometry	•	•	•	•	•
$\pi_2 = Re_l = (\rho vD/\mu)_l$ = inertia/viscous	•	•	•	•	•
$\pi_3 = Fr_l = (v^2/gD)_l$ = inertia/gravity	•	•	•	/•	•
$\pi_4 = Eu_l = (\Delta p/\rho v^2)_l$ = pressure head/inertia	•	•	•	•	•
π_5 = cos ν = orientation with respect to g	•	•	•	/•	•
π_6 = S = slipfactor = v_v/v_l			•	•	•
π_7 = density ratio = ρ_v/ρ_l			•	•	•
π_8 = viscosity ratio = μ_v/μ_l			•	•	•
$\pi_9 = We_l = (\rho v^2 D/\sigma)_l$ = inertia/surface tension			•	/•	•
$\pi_{10} = Pr_l = (\mu Cp/k)_l$		•	•		•
$\pi_{11} = Nu_l = (hD/k)_l$ = convective/conductive		•	•		•
$\pi_{12} = k_v/k_l$ = thermal conductivity ratio			•		•
$\pi_{13} = Cp_v/Cp_l$ = specific heat ratio			•		•
$\pi_{14} = \Delta H/h_{lv}$ = enthalpy number = X = quality		•	•	•	•
$\pi_{15} = Mo_l = (\rho_l \sigma^3/\mu_l^4\, g)$ = capillarity/buoyancy			•	/•	•
$\pi_{16} = Ma = v/(\partial p/\partial \rho)^{1/2}_s$			•	•	•
$\pi_{17} = (h/k_l)(\mu_l^2 g)^{1/3}$			•		•
$\pi_{18} = L^3 \rho_l^2\, g\, h_{lv}/k_l \mu_l (T-T_o)$			•		•

One-g is not the upper limit in gravitational scaling: higher g-values can be obtained during special aircraft trajectories, or in a centrifuge.

Unfortunately, even in single-phase systems scaling is all except simple, as flow and heat transfer are equivalent in model and original (prototype) system only if the corresponding velocity, temperature and pressure fields are identical. Dimensionless numbers can be derived either from the conservation equations for mass, momentum and energy or from similarity considerations, based on dimension analysis. The above identity of velocity, temperature and pressure fields is obtained if all dimensionless numbers are equal in model and prototype.

Scaling two-phase systems is more complicated as:
- Apart from above fields, the spatial distribution (void and flow pattern) is to be considered.
- Geometric scaling often has no sense if the characteristic sizes, e.g. bubble diameter and surface roughness, are almost independent of system dimensions.
- There is a proportion problem, arising from two-phase flow and boiling heat transfer high power density levels.

3-3. Similarity Considerations/Dimension Analysis

Similarity considerations, discussed in detail in Delil, 1991 & 1998, led to the identification of 18 dimensionless numbers (π-numbers) which are relevant for thermal gravitational scaling of two-phase loops. The 18 π-numbers are listed in table 1, showing the relevance of π-numbers in the various sections of the different two-phase systems, schematically depicted in the figures 1 to 3.

As said before, perfect similitude between model and prototype is obtained if all dimensionless numbers are identical in prototype and model. Then there is perfect similitude and only then the scaling is perfect. It is evident that perfect scaling is not possible in the case of two-phase flow and heat transfer: the phenomena are too complex, the number of important parameters or π-numbers is too large. Fortunately also imperfect (distorted) scaling can give useful results. Therefore a careful estimation of the relative magnitudes of the different effects is required. Effects of minor importance in two-phase systems are Mach number in incompressible flow in liquid lines, and Froude number (gravity) in pure vapour flow.

Finally it is remarked that in scaling a two-phase heat transport system:
- Geometric distortion is not permitted to study boundary layer effects and boiling, as identity of surface roughness in prototype and model is to be guaranteed.
- Geometrical distortion is a must when the length scaling leads to not practically small (capillary) conduits in the model, in which the flow phenomena basically differ from flow in the full size prototype.

Sometimes it is more convenient to replace quality X by the volumetric vapour (void) fraction α:

$$(1 - \alpha)/\alpha = S\,(\rho_v/\rho_l)\,/\,(1- X)/X\,. \qquad (1)$$

It is clear that the set of π-numbers presented is rather arbitrary one, e.g. several numbers contain only liquid properties. These numbers can be easily transferred into vapour properties containing numbers using π_6, π_7 and π_8. Similarly π_1 can be used to interchange characteristic length (e.g. duct length, bend curvature radius) and a characteristic diameter (e.g. duct diameter, hydraulic diameter, but if desired also surface roughness/bubble diameter). Sometimes it might be convenient to simultaneously consider two geometric π_1 numbers: one for the overall channel (channel diameter versus length or bend radius), the other pertaining to other parameters (the ratio surface roughness and bubble diameter to investigate boiling heat transfer, or the ratio of surface roughness and channel diameter to study friction pressure drop).

Generally speaking, combinations of π-numbers are chosen such that they optimally suit the problem under investigation. Typical examples are:
- The Morton number

$$\pi_{15} = Mo_l = Re_l^{\,4}\,Fr_l\,/\,We^3 = \rho_l\;\sigma^3\,/\,g\,\mu_l^{\,4}. \qquad (2)$$

It is especially useful for scaling two-phase flow with respect to gravity, as it contains apart from gravity, only liquid properties and surface tension.
- The Mach number

$$\pi_{16} = Ma = v/(\partial p/\partial \rho)^{1/2}, \qquad (3)$$

when compressibility effects are important (e.g. choking strongly depends on homogeneous two-phase quality).
- The Boiling number

$$\pi_{14} = Bo = Q\,/\,\dot{m}\,h_{lv} = \Delta H\,/\,h_{lv}. \qquad (4)$$

Q is the power fed to the boiling liquid. This number appears in the expression for the dimensionless enthalpy at any z in a line heated from outside

$$\Delta H(z)\,/\,h_{lv} = \Delta H_{in}\,/\,h_{lv} + \pi\,D\,z\,q\,/\,\dot{m}\,h_{lv}. \qquad (5)$$

q is heat flux. For sub-cooled or heated liquid it is:

$$\pi_{14} = Q\,/\,\dot{m}\;Cp_l\;\Delta T. \qquad (6)$$

ΔT is the temperature drop. This implies that, if the dimensionless entrance enthalpies are equal for different fluids in similar geometry, equal boiling numbers ensure equal dimensionless enthalpy at similar axial locations. In thermodynamic equilibrium it means equal quality at similar locations and similar sub-cooling/boiling length.
- The condensation number

$$\pi_{17} = (h\,/\,k_l)\,(\mu_l^{\,2}/\,g\;\rho_l^{\,2})^{1/3}. \qquad (7)$$

h is the local heat transfer coefficient.
- The vertical wall condensation number

$$\pi_{18} = L^3\rho_l^{\,2}\,g\,h_{lv}\,/\,\mu_l\,k_l(T- T_o). \qquad (8)$$

T_0 is local sink, T local saturation temperature.

A first step in a practical approach to scale two-phase heat transport systems is the identification of the important physical phenomena, in order to obtain the π-numbers for which identity in prototype and model must be required to realise perfect scaling according to Buckingham´s theorem. Distortion will be permitted for π-numbers pertaining to phenomena considered less important. That the important phenomena and the relevant π-numbers will be different in different parts of a system is obvious. Table 1 shows the relevance (• means relevant) of the π-numbers in the various loop sections.

For refrigerants like ammonia and R114, forced convection heat transfer overrules conduction completely, hence π_{10} π_{11} and π_{12} are not critical in gravitational scaling. π_{16} can be neglected also, since the system maximum power level and line diameters correspond with flow velocities far below the sonic velocity in all parts of the systems including the two-phase sections.

Considering π_3/π_5, it can be remarked that inertia overrules buoyancy not only in pure vapour flow or in a low gravity environment, but also for horizontal liquid sections on earth ($\nu \rightarrow \pi/2$). This implies that there is π-number identity for these sections in low-g prototype and in a terrestrial model, for a horizontal arrangement of these sections. Also it can be remarked that, in the porous (liquid) part of a capillary evaporator, surface tension forces ($2\sigma/D_p$) are dominant over inertia ($\pi_9 \rightarrow 0$), and consequently the evaporator exit quality will approach 1 (pure vapour). This means that gravity is not important for the vapour part of the evaporator and for the vapour line connecting evaporator and condenser.

Important conclusions can be drawn now:
The condensers and, in the mechanically pumped

system also the two-phase lines, are crucial in scaling with respect to gravity. They determine the conditions for the evaporators and single-phase sections. The latter can be scaled in the classical way presented in textbooks.

In the adiabatic two-phase lines (in the mechanically pumped mode) under low-gravity conditions only shear forces are expected to cause the separation of the phases in the high-quality (above say 0.8) mixture, leading to pure annular flow (a fast moving vapour in the core and a by frictional drag induced slowly moving liquid annulus at the inner line wall) for the lower flow rates. For increasing power, hence flow rate, the slip factor increases, introducing waves on liquid-vapour interface and entrainment of liquid in the vapour: so-called wavy annular/ mist flow. Similar flow pattern behaviour can be predicted for vertical downward flow on earth, as it easily can be derived from the flow pattern map for downward two-phase flow (Fig. 8), taken from Oshinowo and Charles (1974), in which water properties at 20 °C must be used to determine the scale of the abscissa.

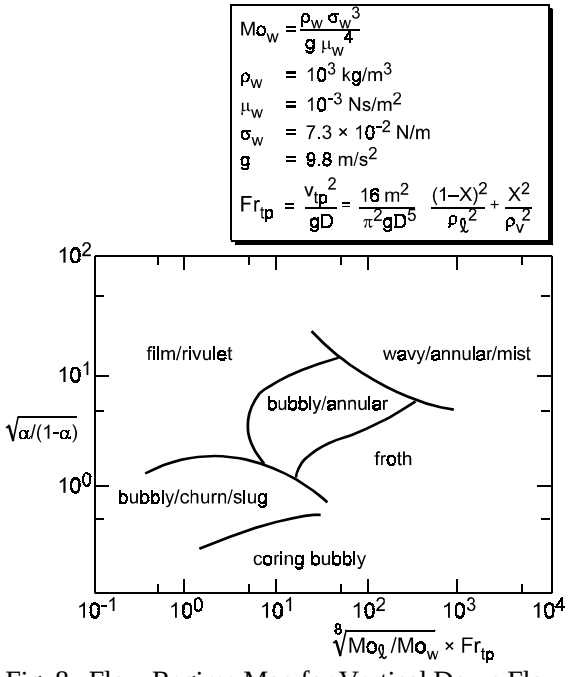

Fig. 8. Flow Regime Map for Vertical Down Flow

The Froude number for two-phase flow used in this figure is defined as:

$$Fr_{tp} = (16\,\dot{m}^2/\pi^2 D^5 g)[X^2/\rho_v^2 + (1-X)^2/\rho_l^2] \quad (9)$$

Comparing low-g and vertical down-ward terrestrial flow, one has to correct the latter for the reduction of the slip factor by the gravity forces assisting the down- flowing liquid layer. Anyhow, vertical down-flow is the preferred two-phase line orientation in the terrestrial model because of the axial-symmetric flow pattern. A similar conclusion can be drawn for the straight tube condenser. Recalling figures 5 to 7, it is remarked that in these condensers the flow will change from wavy/ annular/mist to pure liquid flow, passing different flow patterns, depending on the condensation path.

3-4. Scaling Examples and Possible Experiments

Consequences of scaling are elucidated by the figures 9 and 10, showing the temperature dependence of $g.Mo_l$ or $\rho_l\sigma^3/\mu_l^4$ and $(\sigma/\rho_l)^{½}$ or $D(g.Fr/We)^{½}$.

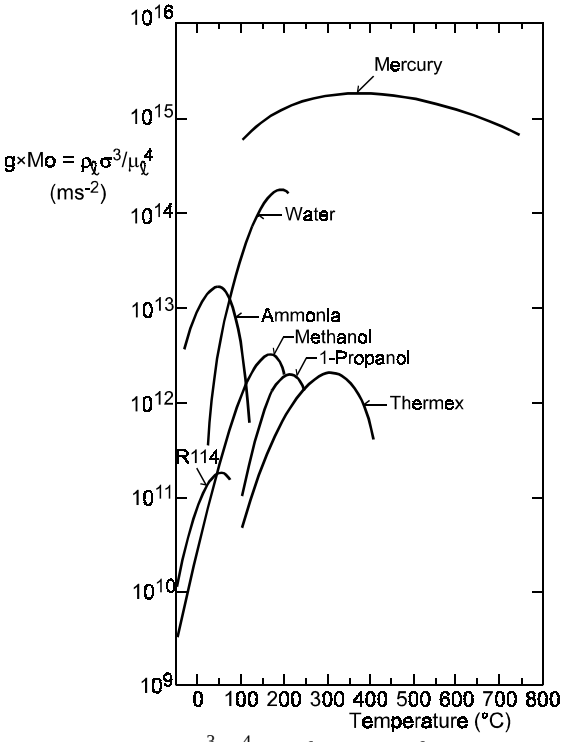

Fig. 9. $g.Mo_l$ or $\rho_l\sigma^3/\mu_l^4$ as a function of temperature

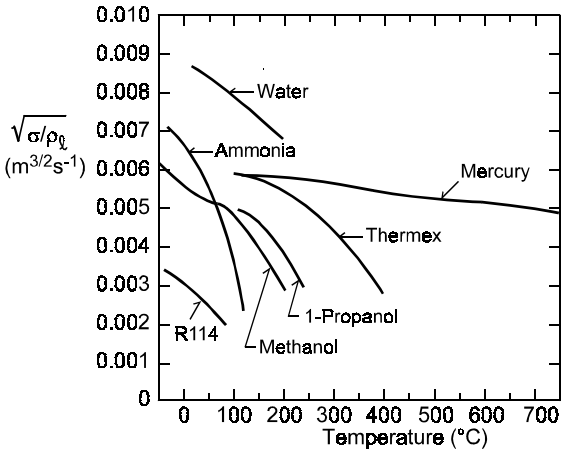

Fig. 10. $\sqrt{\sigma/\rho_\ell}$ as a function of temperature

In case of scaling at the same gravity level, it can

be seen , in figure 9, that the value $\rho_l \sigma^3/\mu_l^4 = 2*10^{12}$ m/s^2 can be realised by seven systems, i.e. a 115°C ammonia, 115°C methanol, 35°C water, 180°C propanol, 235°C propanol, 250°C thermex and a 350°C thermex system. Requiring, in addition to Morton Number identity, also the identity in $(We/Fr)^{½}$, in other words $D/(\sigma/\rho_l)^{½}$, the length scales of the seven systems derived from the corresponding (σ/ρ_l)-values in figure 10, turn out to be proportional to each other with ratios 2.5: 4.5: 8.4: 4.2: 3.0: 5.0: 3.6. Hence the maximum scaling ratio obtainable equals 8.4/2.5 ≈ 3, indicating that geometry scaling at the same gravity level can cover only a limited range.

In addition, scaling of high pressure (say 110 °C) ammonia system parts by low pressure (say -50 °C) ammonia system parts might be attractive for safety reasons or to reduce the impact of earth gravity in vertical two-phase sections. In a similarly manner as the above, one can straightforwardly derive from figure 10, that the length scale ratio between high-pressure prototype and the low-pressure model (characterised by $\rho_l \sigma^3/\mu_l^4 = 2.10^{12}$ m/s^2) is $L_p/L_m = [(\sigma/\rho_l)_p/\sigma/\rho_l)_m]^{1/2} \approx 0.4$. For ammonia such a scaling can be attractive only for sections without heat transfer, since otherwise it will certainly lead to unacceptable high power levels in the model system evaporators and condensers.

Figure 9 shows that the scaling with respect to gravity is restricted to say two decades, if the fluid in prototype and model is the same, e.g. a 10^{-2} g, 80 °C, thermex prototype can be scaled by a 300 °C thermex model on earth. Length scaling: $L_p/L_m = D_p/D_m = (g_m/g_p)^{½}(\sigma/\rho_l)_p^{½}/(\sigma/\rho_l)_m^{½} \approx 14$.

The figure also shows that a very attractive pure geometric scaling application is the scaling of a Mars or Moon base ammonia prototype system by a terrestrial ammonia model, of slightly larger dimensions ($D_m / D_p < 1.5$). This scaling is almost perfect, not only for vertical down-flow but also for horizontal separated flow. In addition, vertical prototype lines can even be simulated by equal geometry model lines that are inclined with respect to the Earth gravity factor. This is due to the relatively small differences between the gravity level on the Earth, Mars and Moon.

Interesting is fluid to fluid scaling: e.g. alkali metal terrestrial prototypes can be scaled by various model systems in space, a 400°C mercury prototype:
- At 10^{-2} g, by a 35°C ammonia model ($L_m/L_p \approx 11$) or 80°C water model ($L_m/L_p \approx 14$).
- At 10^{-4} g, by a methanol model at 35°C ($L_m/L_p \approx 95$), a 130°C thermex ($L_m/L_p \approx 100$), a 30°C R114 ($L_m/L_p \approx 45$).

The remarks made for the pure geometric scaling of Mars and Moon base systems, can be repeated for fluid to fluid scaling: Such planetary two-phase systems can be scaled (almost) perfectly by terrestrial models because of the relatively small differences in gravity levels.
It is remarked that space-oriented mercury systems must be scaled on by other fluid systems in centrifuges on earth.
In addition it can be said that a 25°C R114 prototype at 10^{-2} g can be scaled by a 25°C, 1 g ammonia model ($L_p/L_m \approx 5$), important for the ESA developments discussed next.

To support ESA two-phase activities (TPX I and TPHTS), experiments had to be carried out using the NLR two-phase test rig. This ammonia rig, having approximately the same line diameter as the TPX I loop, has been used for:
- Testing and calibration of TPX I & II and components.
- The scaling of low-g adiabatic and condensing flow as discussed in the following sections: terrestrial, low temperature, vertical down-flow minimises the impact of gravity, hence simulates low-gravity conditions the best.
In addition it is recalled that the full size low-gravity (< 10^{-2} g) mechanically-pumped R114 ESA TPHTS can be adequately scaled by the above ammonia test rig, since:
- The, say 10^{-2} - 10^{-3} g, R114 prototype and the terrestrial ammonia model have approx. identical Morton number.
- This fluid to fluid scaling leads towards the corresponding length scaling $D_p/D_m = (g_m/g_p)^{½} * (\sigma/\rho_l)^{½}_p / (\sigma/\rho_l)^{½}_m \approx 4.5$ to 6.5, which is in agreement with the ratio of the actual diameters, 21 mm for the R114 space-oriented prototype and 4.93 mm for the terrestrial ammonia model.

In summary: Scaling of two-phase heat transport systems is very complicated. Distorted scaling (Murphy, 1950) offers possibilities, especially when not the entire loop but only loop sections are involved. Scaling with respect to gravity is not discussed in literature. Some possibilities can be identified, though for typical and very limited conditions only. The mechanically pumped NLR two-phase ammonia test rig offers: opportunities to scale a TPX I ammonia loop and a very promising application: the terrestrial scaling of an ESA mechanically pumped TPHTS (R114) flight unit. The scaling possibilities for Mars and Moon base systems are very promising.

3-5. Modelling Two-Phase Pressure Drop

An important quantity to be measured during two-phase flow experiments is the pressure drop in adiabatic sections and in condensers: sections considered crucial for two-phase system modelling and scaling. Therefore we will concentrate in the following on the modelling of pressure drops in condensing and adiabatic flow. We will restrict the discussion to straight tubes.

The total local (z-dependent) pressure gradient for annular two-phase flow is the sum of the contributions of friction, momentum and gravity:

$$(dp(z)/dz)_t = (dp(z)/dz)_f + (dp(z)/dz)_m + (dp(z)/dz)_g \quad (10)$$

Following Delil (1991, 1992) and Soliman et al. (1968), elaborate publications on the subject, one obtains for the contribution of friction (deleting the z-dependence to shorten the notation):

$$(dp/dz)_f = - (32\dot{m}^2/\pi^2\rho_v D^5)(0.045/Re_v^{0.2})[X^{1.8} + 5.7(\mu_l/\mu_v)^{0.0523}(1-X)^{0.47}X^{1.33}(\rho_v/\rho_l)^{0.261} + 8.1(\mu_l/\mu_v)^{0.105}(1-X)^{0.94}X^{0.86}(\rho_v/\rho_l)^{0.522}]. \quad (11)$$

X is the local quality X(z), Re_v is the Reynolds number

$$Re_v = 4\,\dot{m}/\pi\, D\, \mu_v\,. \quad (12)$$

The fluid properties μ_l, μ_v, ρ_l and ρ_v are assumed to be independent of z, as they depend only on the mixture temperature, usually being almost constant in adiabatic and condensing sections.

The momentum constituent can be written as

$$(dp/dz)_m = -(16\dot{m}^2/\pi^2D^4)\{[2X(1-\alpha)/\rho_v\alpha^2 - \beta(1-X)/\rho_l\alpha + (1-\beta)(1-X)/\rho_l(1-\alpha) + (1-X)/\rho_l(1-\alpha)](dX/dz) + [X^2(1-\alpha)/\rho_v\alpha^3 + (1-X)^2/\rho_l(1-\alpha)^2](d\alpha/dz)\}. \quad (13)$$

α is the z-dependent local void fraction $\alpha(z)$. $\beta = 2$ for laminar liquid flow, $\beta = 1.25$ for turbulent flow. The gravity constituent is

$$(dp/dz)_g = (1-\alpha)(\rho_l-\rho_v)g\cos\nu. \quad (14)$$

$g \rightarrow 0$ for microgravity conditions and $g.\cos\nu$ equals 9.8 m/s^2 for vertical down-flow on Earth, 3.74 m/s^2 for vertical down-flow on Mars and 1.62 m/s^2 on the Moon. α is eliminated in eq. (13) and (14) by inserting eq. (1).

The slip factor S is to be specified. The principle of minimum entropy production (Zivi, 1964) leads to:

$$S = [(1+1.5Z)(\rho_l/\rho_v)]^{1/3} \quad (15)$$

for annular flow, in which the constant Z (according to experiments) is above 1 and below 2, and

$$S = \{(\rho_l/\rho_v)[1+Z'(\rho_v/\rho_l)(1-X)/X]/[1+Z'(1-X)/X]\}^{1/3} \quad (16)$$

for real annular-mist flow, that is annular flow with a mass fraction Z' of liquid droplets entrained in the vapour core. Z' is between 0 for zero entrainment and 1 for complete entrainment. For the limiting cases Z and $Z' \rightarrow 0$, eqs. (15) and (16) become:

$$S = (\rho_l/\rho_v)^{1/3} \quad (17)$$

The latter relation, representing ideal annular flow, will be used here for reasons of simplicity and since it allows a comparison with the results of calculations found in literature. The influence of $Z \neq 0$ and $Z' \neq 0$ is interesting for future investigations. Insertion of eq. (17) into eq. (1) and (11, 13, 14), yields:

$$(dp/dz)_m = - (32\dot{m}^2/\pi^2\rho_v D^5)(D/2)(dX/dz) * [2(1-X)(\rho_v/\rho_l)^{2/3} + 2(2X-3+1/X)(\rho_v/\rho_l)^{4/3} + (2X-1-\beta X)(\rho_v/\rho_l)^{1/3} + (2\beta-\beta X-\beta/X)(\rho_v/\rho_l)^{5/3} + 2(1-X-\beta+\beta X)(\rho_v/\rho_l)]. \quad (18)$$

$$(dp/dz)_g = (32\dot{m}^2/\pi^2\rho_v D^5)\{1-[1+(\rho_v/\rho_l)^{2/3}(1-X)/X]^1\} * [\pi^2 D^5 g\cos\nu(\rho_l-\rho_v)\rho_v/32\dot{m}^2]. \quad (19)$$

To solve eqs. (11, 18, 19) an extra relation is necessary, defining the z-dependence of X. A relation often used

$$dX/dz = -X_{entrance}/L_c \quad (20)$$

(L_c being the condensation length), means uniform heat removal (hence a linear decrease of vapour quality along the duct), which may be unrealistic. It is better to use

$$\dot{m}\, h_{lv}(dX/dz) = - h\pi D[T(z)-T_s]\ , \quad (21)$$

relating local quality and heat transfer. h is the local heat transfer coefficient h(z), for which one can write

$$h = 0.018\,(k_l\,\rho_l^{1/2}/\mu_l)\,Pr_l^{0.65}\,|-(dp/dz)_t|^{1/2}\,D^{1/2}. \quad (22)$$

This equation, derived, by Soliman et al. (1968), assumes that the major thermal resistance is in a laminar sub-layer of the turbulent condensate film. As already mentioned the two-phase flow path is almost isothermal, which implies constant temperature drop $T(z) - T_s$ (for constant sink temperature T_s), constant fluid properties and a constant Prandtl number, defined by

$$Pr_l = (Cp_l \mu_l)/ k_l. \quad (23)$$

The total condensation pressure drop is

$$\Delta p_t = \int_0^{L_c} (dp/dz)_t dz. \quad (24)$$

Eqs. (10, 11, 18, 19, 21) and eq. (22) can be combined, yielding an implicit non-linear differential equation in the variable X(z), which can be rewritten into a solvable standard form for differential/ algebraic equations

$$F(dX/dz, X) = 0. \quad (25)$$

3-6. Quantitative Examples

Comparing adiabatic ammonia pressure gradient constituents at two temperatures, calculated according to the equations presented above (Fig. 11), proves that the gravity constituent is overruled by the others at low temperature (Delil, 1991). This means that low-g behaviour can be investigated by terrestrial tests at low temperature.

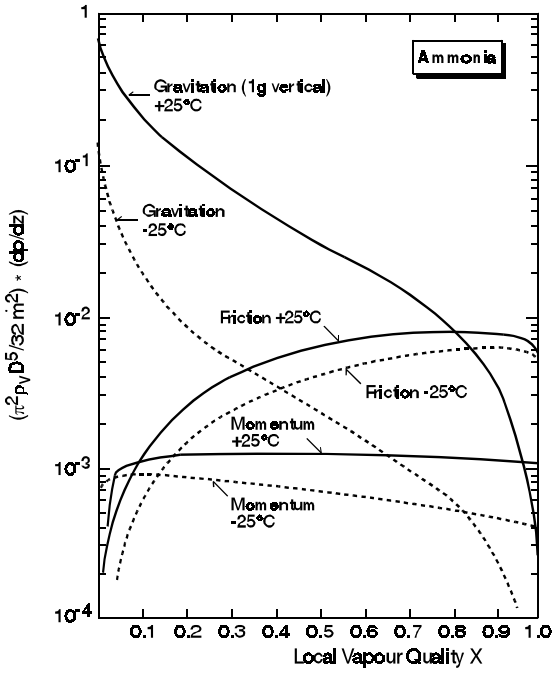

Fig. 11.Vapour Quality Dependence of the Various Constituents of the Local Pressure Gradient

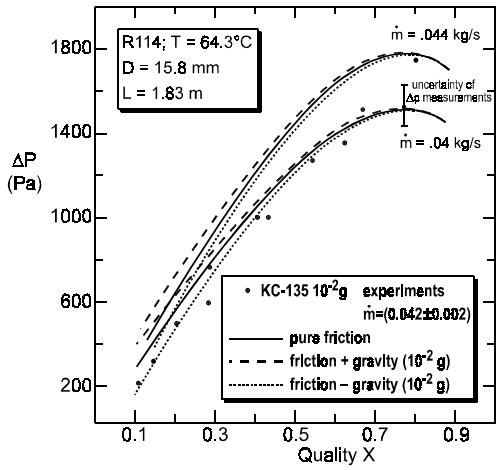

Fig. 12. Measured versus Predicted pressure Drops in an Adiabatic R114 Duct

Figure 12 shows that the calculations for adiabatic annular flow pressure gradients confirm the pressure drops over an adiabatic section, that were determined experimentally during low-g aircraft flights with a R114 system (Chen et al., 1991).

Modelling and calculations have been extended from adiabatic towards condensing flow in a straight condenser duct (Delil, 1992) to investigate the impact of gravity level on the duct length required to achieve complete condensation. This impact, which has been reported to lead to duct lengths up to more than one order of magnitude larger for zero gravity as compared to horizontal orientation in Earth gravity (Da Riva, Sanz, 1991), has been assessed (Delil, 1992) for various mass flow rates, duct diameters and thermal (loading) conditions, for two working fluids i.e. ammonia (working fluid for the Space Station, for capillary pumped two-phase systems and for TPX) and R114 (working fluid of the ESA TPHTS).

A summary of results of calculations carried out for ammonia, the most promising working fluid for future two-phase systems, is presented next. To compare the results of the calculations with data from literature, the condenser defined by Da Riva, Sanz (1991), was chosen as the baseline (main characteristics are power Q = 1000 W, line diameter D = 16.1 mm, ammonia temperature T = 300 K and a temperature drop to sink ΔT = 10 K. The other parameter values are listed in the table on next page.

Gravity levels considered are zero gravity g=0, Earth gravity (1-g) g=9.8 m/s^2, Mars gravity g=3.74 m/s^2, Moon gravity g=1.62 m/s^2, and 2-g macro-gravity level 19.6 m/s^2. Illustrative results of calculations are discussed next.

T	(K)	300	243	333
h_{lv}	(J/kg)	$1.16*10^6$	$1.36*10^6$	$1.00*10^6$
$\dot{m}$	(kg/s)	$8.64*10^{-4}$	$7.36*10^{-4}$	$9.98*10^{-4}$
μ_l	(Pa.s)	$1.40*10^{-4}$	$2.47*10^{-4}$	$0.94*10^{-4}$
μ_l/μ_v	(-)	12.30	30.66	8.54
ρ_l	(kg/m^3)	600	678	545
ρ_l/ρ_v	(-)	72.46	652.4	26.6
k_l	(W/m.K)	0.465	0.582	0.394
Pr	(-)	1.42	1.90	1.25

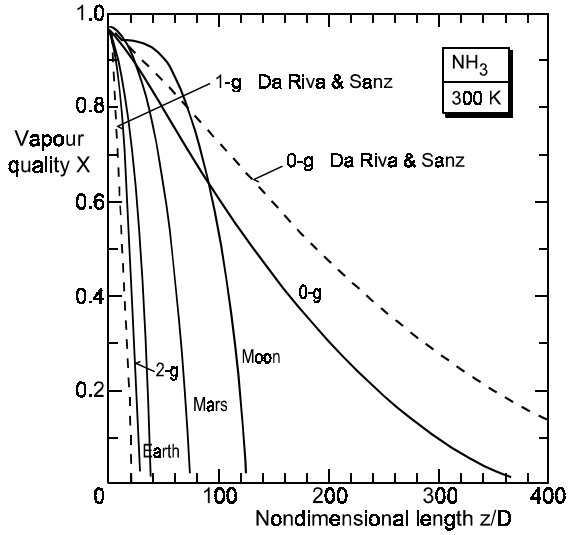

Fig. 13. NH_3, Vapour Quality along 16.1 mm Duct, at 300 K, 1 kW, ΔT = 10 K, for All Gravity Levels

Figure 13 shows the vapour quality X along the condensation path (as a function of the non-dimensional condensation length z/D) for all gravity levels mentioned, including the curves of Da Riva and Sanz (1991), for zero-g and horizontal condensation on earth. The curves start at entrance quality 0.96 for which annular flow, assumed in the modelling, is expected to be established. From this figure it can be concluded that:
- The length required for full condensation strongly increases with decreasing gravity: 0-g condensation length is roughly 10 times the terrestrial one.
- The data presented by Da Riva & Sanz (1991), can be considered as extremes: a horizontal condensation length of say 50% of the terrestrial down-flow length (induced by the stratified flow pattern that enhances the transfer area and heat transfer coefficient) and higher zero-g predictions (induced by the equation for the heat transfer coefficient used, being different from the model presented here).

To assess the impact of the fluid saturation temperature on condensation performance, similar curves have been calculated for two other temperatures, 243 K and 333 K and the above parameter values (Delil, 1992). The calculations show that the full condensation length increases with the temperature for zero gravity conditions, but decreases with temperature for the other gravity levels. This implies that the differences between Earth gravity outcomes and micro-g outcomes decrease with decreasing temperature, confirming the statement already made: the effect of gravity is reduced under lower temperature vertical down-flow conditions.

Calculation of the vapour quality distribution along the 16.1 mm reference duct for condensing ammonia (at 300 K) under Earth gravity and 0-g conditions, for power levels from 0.5 kW up to 25 kW, yielded (Delil, 1992):
- A factor 50 in power, 25 kW down to 500 W, corresponds in a zero gravity environment to a relatively minor reduction in full condensation length, i.e. from say 600 D to 400 D (from 9.5 to 6.5 m).
- Under Earth gravity conditions, power and full condensation length are strongly interrelated: from L_c = 554 D at 25 kW to only 19 D at 500 W.
- The gravity dependence of the full condensation length decreases with increasing power, until the differences vanish at roughly 1 MW condenser choking conditions. The latter value is the upper limit, calculated, following Zivi (1964), for ideal annular flow. Choking may occur at considerably lower power values in case of actual annular-wavy-mist flow, but the value exceeds anyhow the (homogeneous flow) choking limit 170 kW.

Calculation of the vapour quality along the duct for three gravity levels (0, 1, 2-g) and three duct diameters (8.05, 16.1, 24.15 mm) at 300 K, yielded the ratio of the absolute duct lengths L_c(m) needed for full condensation under 0-g and 1-g respectively (Delil, 1992). It has been concluded that the ratio between full condensation lengths in 0-g and 1-g ranges from 1.5 for the 8.05 mm duct, via 11 for the 16.1 mm duct, up to more than 30 for the 24.15 mm duct. In other words, smaller line diameter systems are less sensitive for differences in gravity levels as compared with larger diameter systems. This is confirmed by TPX I flight data (Delil, 1995).

Since the model developed is valid for pure annular flow only, it is worthwhile to investigate the impact of other flow patterns present inside the condenser duct (mist flow at the high quality side, slug and bubbly flow at the low quality side and wavy-annular-mist in between), in other words to investigate whether the pure annular flow assumption, leads towards slightly or substantially

overestimated full condensation lengths. A further complication is the lower boundary of the annular-wavy-mist flow pattern. In addition, flow pattern transitions occur at vapour quality values, which strongly depend on working fluid (temperature) and line diameter.

In summary it can be said that the information presented confirms the results of other models: When designing condensers for space applications one should carefully use and interpret data obtained from terrestrial condenser tests, even when the latter pertain to vertical down-ward flow situations (characterised by the same flow pattern). The model equations given are useful for a better understanding of the problems that can be expected: problems related to flow and heat transfer (necessary lengths of condensers for space applications). The equations and results of calculations suggest that hybrid scaling exercises, combining geometrical and fluid-to-fluid scaling, can beneficently support the design of two-phase heat transport systems for space.
With respect to the local heat transfer equation used, eq. (22), it can be remarked that it has a wrong lower limit $h \rightarrow 0$ for $(dp/dz)_t \rightarrow 0$, which disappears by incorporating conduction through the liquid layer. Preliminary calculations indicate that the incorporation of pure conduction will lead to somewhat shorter full condensation lengths, both for zero-g and for non-zero-g conditions. This implies quantitative changes only, in other words the conclusions presented above remain valid.

4. FLOW PATTERN ASPECTS

Accurate knowledge of the gravity level dependent two-phase flow regimes is crucial for modelling and designing two-phase heat transport systems for space, as flow patterns directly affect thermal hydraulic characteristics of two-phase flow and heat transfer. Therefore gravity level dependent flow pattern (regime) maps are to be created.

Hamme and Best (1997) created, based on many low-gravity aircraft flight data of a R12, 10.5 mm lines experiment, three-dimensional flow pattern maps as shown in the figures 14 and 15. Figure 16 summarises their 0-g data. Figure 17 depicts data of experiments in low-g aircraft with Cyrène, an ammonia system with a 4.7 mm line diameter (Lebaigue et al., 1998). Figure 18 shows the 0-g map, derived from the TPX I VQS flight data.

The above maps partly contradict each other. A comparison between the figures suggests that the annular flow transition occurs in the three systems.

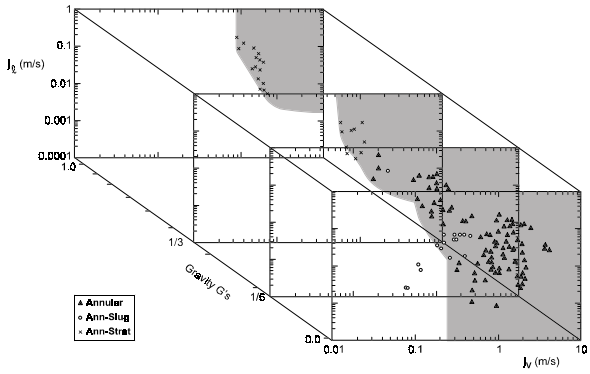

Fig. 14. Gravity Dependent 3-D Annular Flow, Flow Regime Map

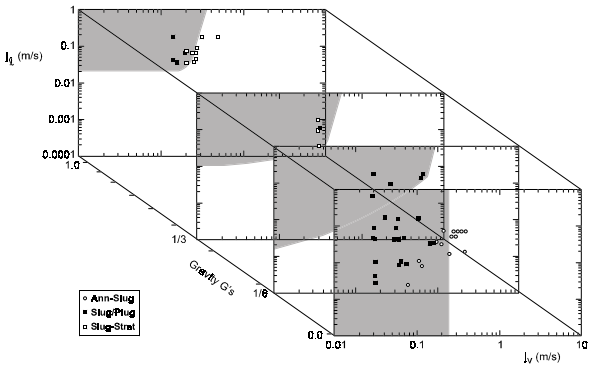

Fig. 15. Gravity Dependent 3-D Slug/Plug Flow, Flow Regime Map

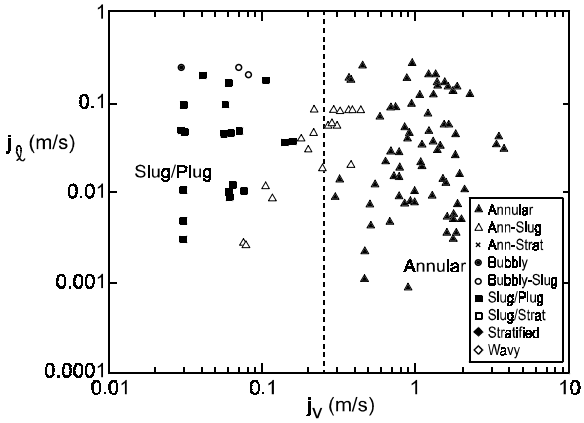

Fig. 16. Zero Gravity Flow Pattern Map

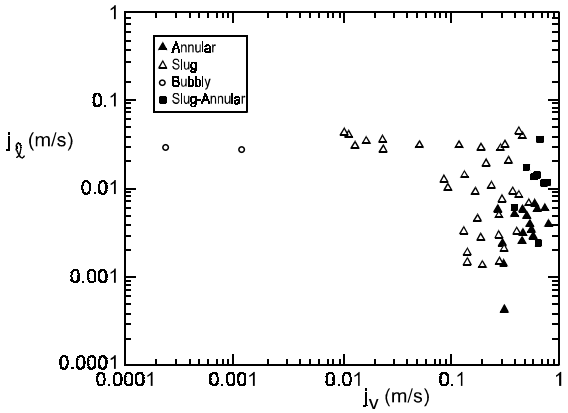

Fig. 17. Cyrène Flow Pattern Map

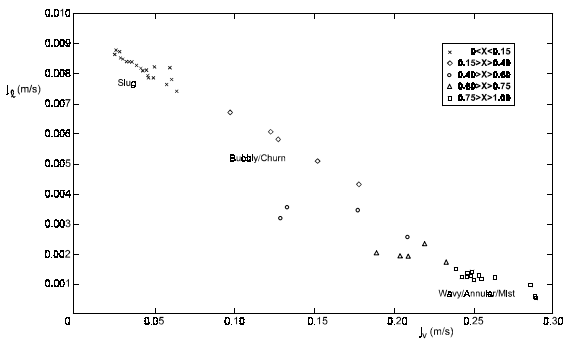

Fig. 18. TPX I Flow Pattern Map

more or less at the same j_v-value 0.2-0.25 m/s, but at different j_l-values. This can be caused either by the different working fluids (R12, ammonia, ammonia) or the different inner line diameter (10.5 mm, 4.7 mm, 4.93 mm).

It is obvious that a lot of work has to be done before complete flow pattern (regime) maps will be produced and become mature, preferably in the normalised format of figure 8 or in the good alternative: the three-dimensional format j_v - j_l - g, like in the figures 14 and 15.

Finally it is stressed again that the situation around the design of ammonia two-phase heat transport system prototypes for Mars and Moon base applications looks very promising, because:
- Planetary gravity flow pattern maps can be easily obtained from measurements in terrestrial model systems with the same or another working fluid, almost equal or even equal geometry, and if necessary with lines having a dedicated angle with the Earth gravity vector, i.e. cos ν = 0.4 (in the Mars case), 0.16 (in the Moon case).
- These maps can be filled with data obtained from experiments with ammonia test loops, carried out during low-gravity aircraft trajectories.

5. PITTING

Pitting corrosion of aluminium alloys is well known in halide containing liquids. It is expected that the non-condensible gas generation found in Al 6061 ammonia heat pipes, with Mg containing AlMg Alloy wicks (Lapinski & Antoniuk, 1991), was due to pitting corrosion.

Pitting corrosion was recently observed on non-passivated (machined) surfaces. in a closed Al 6061-T651 two-phase ammonia loop, containing porous nickel evaporators. Large amounts of pitting corrosion were found on the machined surfaces, some at the weldings. Figure 19 shows corrosion pits. Pitting products surround the pits.

Fig. 19. Pitting on a Machined Surface

The X-ray spectrum (Fig. 20) shows the presence of Nickel inside the corrosion pit. No pitting was observed in the piping itself. The structural integrity of the closed loop was not impaired.

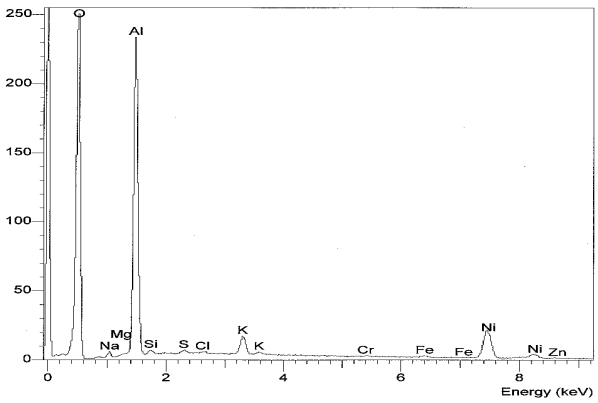

Fig. 20. X-Ray Spectrum of a Corroded Surface

Figure 21 shows the X-ray spectrum of a non-damaged Al 6061 surface. A comparison between the figures 20 and 21 clearly shows the substantial increase in nickel content.

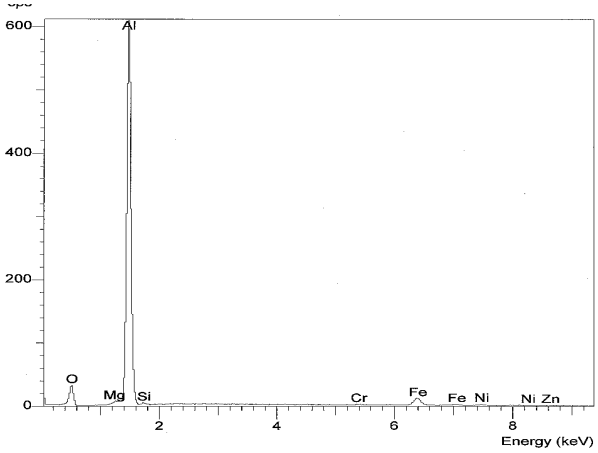

Fig. 21. Spectrum of a Non-Damaged Surface

Corrosion pitting is a local phenomenon. It is associated with a potential difference between a

non-passivated spot (no oxide layer present due to various reasons such as machining, weak oxide layer etc) and its passivated surroundings. Initiation sites for pitting are usually phases in the base material with a different static potential as compared to the matrix. These phases can be cathodic as well as anodic with respect to its surroundings. A cathodic example (an analog of a NaCl-water system) is precipitation of Al_2Cu in Al-alloys with Copper. These precipitates are surrounded by a Copper depleted zone with is anodic to the Al_2Cu precipitate. This anodic zone corrodes selectively. An anodic example are Mg containing Al alloys where the strengthening component is Al_3Mg_2, This precipitate is anodic with respect to the matrix and dissolves. The presence of nobler materials in the closed ammonia loop seems to strongly increase the amount of pitting corrosion of the aluminium alloy. Therefore, far higher amounts of pitting corrosion were found in systems containing a Nickel porous wick (Fig. 20), as compared to systems using a polyethylene wick (Fig. 21).

It is obvious that the phenomenon of pitting corrosion, discovered in Nickel and Stainless Steel containing aluminium/ammonia two-phase loops, indicates that producers of such loops for aerospace applications must be very careful. Since local surface damages can always occur, e.g. a scratch during handling, it is recommended always to cure such a loop with a passivating fluid, before its final filling.

6. CONCLUSION

In conclusion it can be remarked that, due to the results of earth-based research and development and in-orbit technology demonstration, the space-oriented two-phase heat transport technology is becoming mature. Two-phase thermal control systems are getting widely accepted by the aerospace community.

But there still remains a lot of research to be done on several critical issues, being:
- The creation of reliable flow pattern maps for various working fluids, gravity levels, system sizes, etc.
- The extension of the modelling of two-phase pressure drops to non-annular flow regimes, to non-straight tubelines, and to evaporating flow.
- The development of algorithms to interactively determine condensing or evaporating trajectories in the flow pattern maps.
- The prevention of pitting corrosion.

Several outcomes of the above research issues are to be supported by experimenting in low-gravity environments.

Acknowledgement

The author expresses his thanks to:
- The Chairman of the 11th IHPC, Prof. Dr. S. Maezawa, and the Japanese Local Organising Committee, for the kind invitation to present this keynote lecture.
- Dr. A. de Rooij (ESA-ESTEC, Materials and Processes Division) for his valuable contributions to the pitting section.

Nomenclature

A	area	m^2
Bo	boiling number	-
Cp	specific heat at constant pressure	J/kg.K
D	diameter	m
d	diameter of curvature	m
Eu	Euler number	-
Fr	Froude number	-
g	gravitational acceleration	m/s^2
H	enthalpy	J/kg
h	heat transfer coefficient	$W/m^2.K$
h_{lv}	latent heat of vaporisation	J/kg
j	superficial velocity	m/s
k	thermal conductivity	W/m.K
L	length	m
Ma	Mach number	-
Mo	Morton number	-
$\dot{m}$	mass flow rate	kg/s
Nu	Nusselt number	-
p	pressure	Pa, N/m^2
Pr	Prandtl number	-
Q	power	W
q	heat flux	W/m^2
Re	Reynolds number	-
S	slip factor	-
T	temperature	K, ˚C
t	time	s
v	velocity	m/s
We	Weber number	-
X	vapour quality	-
z	axial or vertical co-ordinate	m
α	vapour fraction (volumetric)	-
β	constant in eq. (13)	-
δ	surface roughness	m
Δ	difference, drop	-
μ	viscosity	Ns/m^2
σ	surface tension	N/m
π	dimensionless number	-
ρ	density	kg/m^3
ν	angle (with respect to gravity)	rad

Subscripts

a	acceleration	p	pore/prototype
c	condenser	s	entropy
f	friction	t	total
g	gravitation	tp	two-phase
l, ℓ	liquid	v	vapour
m	momentum, model	w	water
o	reference condition		

References

1. Allen, J.S., Hallinan, K.P., Lekan, J., A Study of the Fundamental Operation of a Capillary Driven Heat Transfer Device in Both Normal and Low Gravity, Part I. Liquid Slug Formation in Low Gravity, AIP Conf. Proc. 420, Space Technology & Applications International Forum, Albuquerque, NM, USA, 1998, pp. 471-477.

2. Allen, J.S., Hallinan, K.P., A Study of the Fundamental Operation of a Capillary Driven Heat Transfer Device in Both Normal and Low Gravity, Part II. Effect of Evaporator Meniscus Oscillations, AIP Conf. Proc. 458, Space Technology & Applications International Forum, Albuquerque, NM, USA, 1999, pp. 811-817.

3. Antar, B.N., Collins, F.G., Flow Boiling in Low Gravity Environment, AIChE Symp. Series 310, Heat Transfer, Houston, TX, USA, 1996, pp. 32-44.

4. Antoniuk, D., Nienberg, J., Analysis of Salient Events in the Two-Phase Thermal Control Flight Experiment, SAE 981817, 28th International Conference on Environmental Systems Danvers, MA, USA, 1998.

5. Bienert, W., Wolf, D., Temperature Control with Loop Heat Pipes: Analytical Model and Test Results, Proc. 9th International Heat Pipe Conference, Albuquerque, USA, 1995, pp. 981-988.

6. Bienert, W.B., Baker, C.L., Ducao, A.S., Loop Heat Pipe Flight Experiment, SAE 981580, 28th International Conference on Environmental Systems, Danvers, MA, USA, 1998.

7. Bousman, W.S., Dukler, A.E., Ground Based Studies of Gas-Liquid Flows in Microgravity Using Learjet Trajectories, AIAA 94-0829, 32nd AIAA Aerospace Sciences Meeting, Reno, NV, USA, 1994.

8. Bousman, W.S., Dukler, A.E., Studies of Gas-Liquid Flow in Microgravity: Void Fraction, Pressure Drop and Flow Patterns, AMD-174/FED-175, Proc. of Symposium on Fluids Mechanics Phenomena in Microgravity, ASME Winter Annual Meeting, New Orleans, LA, USA, 1993, pp. 23-36.

9. Butler, D., Overview of CPL & LHP Applications on NASA Missions, AIP Conf. Proc. 458, Space Technology & Applications International Forum, Albuquerque, NM, USA, 1999, pp. 792-799.

10. Butler, D., Ottenstein, L., Ku, J., Flight Testing of the Capillary Pumped Loop Flight Experiments, SAE 951566, 25th International Conference on Environmental Systems, San Diego, CA, USA, 1995.

11. Carey, P. Van, Liquid-Vapor Phase-Change Phenomena, Hemisphere Publishing Company, Washington DC, USA, 1992.

12. Chen, I. et al, Measurements and Correlation of Two-Phase Pressure Drop under Microgravity Conditions, J. of Thermophysics, 5, 1991, pp. 514-523.

13. Colin.C., Fabre, J., Dukler,A., Gas-Liquid Flow at Microgravity Conditions, Int. J. of Multiphase Flow, 17, 1991, pp. 533-544.

14. Collier, J.G., Convective Boiling and Condensation, McGraw-Hill, Maidenhead, UK, 1972.

15. Crowley, C.J., Sam, R.G., Microgravity Experiments with a Simple Two-Phase Thermal System, 8th Symposium on Space Nuclear Power Systems, AIP Conf. Proc., Space Technology & Applications International Forum, Albuquerque, NM, USA, 1991, pp.1207-1213.

16. Cullimore, B., Capillary Pumped Loop Application Guide, SAE 932156, 23rd International Conference on Environmental Systems, Colorado Springs, USA, 1993.

17. Cullimore, B., Nikitkin, M., CPL and LHP Technologies: What are the differences, What are the similarities? , SAE 981587, 28th International Conference on Environmental Systems, Danvers, MA, USA, 1998..

18. Cykhotsky, V.M., et al., Development & Analyses of Control Methods of the International Space Station Alpha Russian Segment thermal Control System Parameters, AIP Conf. Proc. 458, Space Technology & Applications International Forum, Albuquerque, NM, USA, 1999, pp. 848-853.

19. Da Riva, I., Sanz. A, Condensation in Ducts, Microgravity Science and Technology, 4, 1991, pp. 179-187.

20. Delil, A.A.M., Thermal Gravitational Modelling and Scaling of Two-Phase Heat Transport Systems: Similarity Considerations and Useful Equations, Predictions Versus Experimental Results, NLR TP 91477 U, ESA SP-353, 1st European Symposium on Fluids in Space, Ajaccio, France, 1991, pp. 579-599.

21. Delil, A.A.M., Gravity Dependence of Pressure Drop and Heat transfer in Straight Two-

Phase Heat Transport System Condenser Ducts, NLR TP 92167 U, SAE 921168, 22nd International Conference on Environmental Systems, Seattle, WA, USA, 1992.

22. Delil, A.A.M. et al., TPX for In-Orbit Demonstration of Two-Phase Heat Transport Technology - Evaluation of Flight & Postflight Experiment Results, NLR TP 95192 U, SAE 95150, 25th International Conference on Environmental Systems, San Diego, CA, USA, 1995.

23. Delil, A.A.M., Dubois, M., Supper, W., The European Two-Phase Experiments: TPX I & TPX II, NLR TP 97502 U, 10th International Heat Pipe Conference, Stuttgart, Germany, 1997.

24. Delil, A.A.M., 1998, Two-Phase Heat Transport Systems for Space: Thermal Gravitational Modelling & Scaling, Similarity Considerations, Equations, Predictions, Experimental Data and Flow Pattern Mapping, NLR TP 98268, SAE 981692, 28th International Conference on Environmental Systems, Danvers, MA, USA, 1998.

25. Fore, L.B., Witte, L.C., McQuilen, J.B., Microgravity Heat Transfer and Pressure Drop in Gas Liquid Mixtures: Slug and Annular Flow, AIChE Symposium Series 310, Heat Transfer, Houston, TX, USA, 1996, pp. 45-51.

26. Grigoriev, Y.I., et al., Two-Phase Thermal Control System of International Space Station Alpha Russian Segment, Proc. Int. Workshop Non-Compression Refrigeration & Cooling, Odessa, Ukraine, 1999, pp.73-83.

27. Grigoriev, Y.I., et al., Two-Phase Heat Transfer Loop of Central Thermal Control System of the International Space Station Alpha Russian Segment, AIChE Symp. Series 310, Heat Transfer, Houston, TX, USA, 1996, pp. 9-18.

28. Hagood, R., CCPL Flight Experiment: Concepts through Integration, SAE 981694, 28th International Conference on Environmental Systems, Danvers, MA, USA, 1998.

29. Hamme, T.A., Best, F.R., Gravity Dependent Flow Regime Mapping, AIP Conf. Proc. 387, Space Technology & Applications International Forum, Albuquerque, NM, USA, 1997, pp. 635-640.

30. Huckerby, C.S., Rezkallah, K.S., Flow Pattern Obsevations in Two-Phase Gas-Liquid Flow in a Straight Tube under Normal and Microgravity Conditions, Proc. 1992 AIChE Heat Transfer Conference, San Diego, CA, USA, pp. 139-147.

31. Jayawardena, S.S., Reduced Gravity Two-Phase Flow at Tee Junction, AIChE Symp. Series 310, Heat Transfer, Houston, TX, USA, 1996, pp. 68-72.

32. Kawaji, M., Westbye, C.J., Antar, B.N., Microgravity Experiments on Two-Phase Flow and Heat Transfer during Quenching of a Tube and Filling a Vessel, 27th AIChE Symp. Series 283, 1991, pp. 45-51.

33. Kaya, T., Ku, J., A Parametric Study of Performance Characteristics of Loop Heat Pipes, SAE 1999-01-2006, Proc. 29th International Conference on Environmental Systems, Denver. CO, USA, 1999.

34. Kim, J.H., et al., The Capillary Pumped Loop III Flight Demonstration, Description, and Status, AIP Conf. Proc. 387, Space Technology & Applications International Forum, Albuquerque, NM, USA, 1997, pp. 623-628.

35. Ku, J., Ottenstein, L., Butler, D., 1996, Performance of CAPL 2 Flight Experiment, SAE 961431, 26th International Conference on Environmental Systems, Monterey, CA, USA, 1996.

36. Ku, J., Operating Characteristics of Loop Heat Pipes, SAE 1999-01-2007, Proc. 29th International Conference on Environmental Systems, Denver. CO, USA, 1999.

37. Lapinski, R.J., Antoniuk, D., Characterization of Aging Mechanisms in Aluminum/Ammonia Heat Pipes, AIAA 91-1361, AIAA 26th Thermo-physics Conference, Honolulu, HI, USA, 1991.

38. Lebaigue, O., Bouzou, N., Colin, C., Cyrène: An Experimental Two-Phase Ammonia Fluid Loop in Microgravity. Results of a Parabolic Flight Campaign, SAE 981689, 28th International Conference on Environmental Systems, Danvers, MA, USA, 1998.

39. Leontiev, A.I., et al., Thermophysics of Two-Phase Flows in Microgravity: Russian-American Research Project, AIP Conf. Proc. 387, Space Technology & Applications International Forum, Albuquerque, NM, USA, 1997, pp. 541-546.

40. Maidanik, Y., Fershtater, Y., Goncharov, K., Capillary Pump Loop for Systems of Thermal Regulation of Spacecraft, ESA SP 324, Proc.4th European Symposium on Space Environmental Control Systems, Florence, Italy, 1991, pp. 87-92.

41. Maidanik, Y.F., Solodovnik, N., Fershtater, Y.G., Investigation of Dynamic and Stationary Characteristics of Loop Heat Pipe, Proc. 9th International Heat Pipe Conference Albuquerque, NM, USA, 1995, pp. 1000-1006.

42. Mayinger, F., Strömung und Wärmeübergang in Gas-Flüssigkeits-Gemischen, Springer Verlag Wien, Austria, 1982.

43. McQuilen, J.B., Neumann, E.S., Two-Phase Flow Research Using the Learjet Apparatus, NASA TM-106814, 1995.

44. Miller-Hurlbert, K., The Two-Phase Extended Evaluation in Microgravity Flight Experiment:

Description and Overview, AIP Conf. Proc. 387, Space Technology & Applications International Forum, Albuquerque, NM, USA, 1997, pp. 547-54.
45. Miller, K., et al., Microgravity Two-Phase Pressure Drop Data in Smooth Tubing, AMD-174/FED-175, Proc. Symposium on Fluids Mechanics Phenomena in Microgravity, ASME Winter Annual Meeting, New Orleans, LA, USA, 1993, pp.37-50.
46. Murphy, G., Similitude in Engineering, Ronald Press, New York, USA, 1950.
47. Orlov, A.A., et al., The Loop Heat Pipe Experiment Onboard the Granat Spacecraft, 6th European Symposium on Space Environmental Control Systems, Noordwijk, Netherlands, ESA SP400, 1997, pp. 341-353.
48. Oshinowo, T., Charles, M.E., Vertical Two-Phase Flow, Flow Pattern Correlations, Can. J. Chem. Engng., 52, 1974, pp. 25-35.
49. Ottenstein, L., Nienberg, J., Flight Testing of the Two-Phase Flow Flight Experiment, SAE 981816, 28th Int. Conference on Environmental Systems, Danvers, MA, USA, 1998.
50. Reinarts, T.R., Ungar, E.K., Prediction of Annular Two-Phase Flow in Microgravity and Earth-Normal Gravity, AIChE Symposium Series 310, Heat Transfer, Houston, TX, USA, 1996, pp. 32-44.
51. Reinarts, T.R., Ungar, E.K., Butler, C.D., Adiabatic Two-Phase Pressure Drop in Microgravity: TEMP2A-3 Flight Experiment Measurements and Comparison with Predictions, AIAA 95-0635, 33rd AIAA Aerospace Sciences Meeting, Reno, NV, USA, 1995.
52. Reinarts, T.R., Adiabatic Data and Modeling for Zero and Reduced (Horizontal Flow) Acceleration Fields, Ph.D. Dissertation, Texas A&M University, 1993.
53. Rite, R.W., Rezkallah, K.S., Heat Transfer in Two-Phase Flow Through a Circular Tube at Reduced Gravity, J. of Thermophysics and Heat Transfer, 8(4), 1994, pp. 702-708.
54. Soliman, M., Schuster, J.R., Berenson, P.J., A General Heat Transfer Correlation for Annular Flow Condensation, Trans. ASME, J. of Heat Transfer, 90, 1968, pp. 267-276.
55. Stenger, F.J., Experimental Study of Water-Filled Capillary Pumped Heat Transfer Loops, NASA TMX-1310, 1966.
56. Ungar, E.K., Mai, T.D., The Russian Two-Phase Thermal Control System for the International Space Station, AIChE Symposium Series 310, Heat Transfer, Houston, TX, USA, 1996, pp. 19-24.
57. Wallis, G.B., One-dimensional Two-phase Flow, McGraw-Hill,New York,USA, 1969
58. Wőlk, G., Dreyer, M., Rath, H.J., Investigation of Two-Phase Flow in Small Diameter Non-Circular Channels under Low and Normal Gravity, AIP Conf. Proc.420, Space Technology & Applications International Forum, Albuquerque, NM, USA, 1999, pp. 785-791.
59. Zhao, L., Rezkallah, K.S., Gas-Liquid Flow Patterns at Microgravity Conditions, Int. J. of Multiphase Flow,19, 1993, pp. 751-763.
60. Zivi, S.M., Estimation of Steady-State Void Fraction by Means of the Principle of Minimum Entropy Production, Trans. ASME, J. Heat Transfer, 86, 1964, pp. 247-252.